SUPPORTING INFORMATION

Exploring Host-Guest Interactions in the α-$Zn_3(HCOO)_6$ Metal-Organic Framework

Bowei Wu,[a] Y. T. Angel Wong,[a] Bryan E. G. Lucier,[a] Paul D. Boyle,[a] Yining Huang[a,*]

[a]*Department of Chemistry, The University of Western Ontario, 1151 Richmond Street, London, Ontario, Canada, N6A 5B7*

*Corresponding author: Yining Huang (yhuang@uwo.ca)

Table of Contents

Table S1. Summary of crystallographic data for CO_2-loaded α-$Zn_3(HCOO)_6$.

Formula	$C_{6.25}H_6O_{12.50}Zn_3$
Formula Weight [g/mol]	477.22
Crystal Color and Habit	colourless prism
Crystal System	monoclinic
Space Group	P 2_1/n
Temperature [K]	120
a [Å]	11.3261(15)[a]
b [Å]	9.8210(14)[a]
c [Å]	14.4412(19)[a]
α [°]	90
β [°]	91.297(5)[a]
γ [°]	90
V [Å^3]	1605.9(4)[a]
Z	4
F(000)	934
ρ [g/cm]	1.974
λ(CuKα) [Å]	1.54178
μ [cm^{-1}]	5.787
Max 2θ for data collection [°]	135.17
Measured fraction of data	0.973
Number of reflections measured	5024
Unique reflections measured	5024
R_1	0.0303
wR_2	0.0986
R_1 (all data)	0.0306
wR_2 (all data)	0.0992
GOF	1.224

[a]Errors are given in parentheses

$R_1 = \Sigma(|F_o| - |F_c|) / \Sigma F_o$

$wR_2 = [\Sigma(w(F_o^2 - F_c^2)^2) / \Sigma(w F_o^4)]^{½}$

GOF = $[\Sigma(w(F_o^2 - F_c^2)^2) / (\text{No. of reflns.} - \text{No. of params.})]^{½}$

Table S2. Atomic coordinates for CO_2-loaded α-$Zn_3(HCOO)_6$ obtained from X-ray diffraction. Errors are given in parentheses.

Atom[a]	x	y	z	$U_{iso/equiv}$
Zn1	0.24331(4)	0.07756(5)	0.36832(3)	0.00978(16)
Zn2	0.24050(4)	0.39126(5)	0.31300(3)	0.01070(16)
Zn3	0.5000	0.0000	0.5000	0.01207(19)
Zn4	0.0000	0.0000	0.5000	0.01229(19)
O1	0.3157(2)	-0.0274(3)	0.47692(18)	0.0137(6)
C1	0.2572(4)	-0.1057(4)	0.5306(3)	0.0139(8)
O2	0.1496(2)	-0.1141(3)	0.5339(2)	0.0171(6)
O3	0.1025(2)	0.1551(3)	0.43955(18)	0.0124(5)
C2	0.0706(4)	0.2786(4)	0.4488(3)	0.0157(8)
O4	0.1118(2)	0.3792(3)	0.40880(19)	0.0163(6)
O5	0.1919(2)	0.1994(3)	0.25419(18)	0.0120(5)
C3	0.1699(3)	0.1720(4)	0.1697(3)	0.0133(8)
O6	0.1833(2)	0.0606(3)	0.13111(19)	0.0155(6)
O7	0.3472(2)	0.2554(3)	0.39048(19)	0.0123(6)
C4	0.4222(4)	0.2883(4)	0.4533(3)	0.0165(8)
O8	0.4814(2)	0.2092(3)	0.5024(2)	0.0189(6)
O9	0.1494(2)	-0.0832(3)	0.30488(18)	0.0125(5)
C5	0.0458(4)	-0.1294(4)	0.3133(3)	0.0157(8)
O10	-0.0234(2)	-0.1044(3)	0.3761(2)	0.0189(6)

O11	0.3700(2)	-0.0069(3)	0.28039(18)	0.0122(6)
C6	0.4814(3)	-0.0149(4)	0.2878(3)	0.0136(8)
O12	0.5411(2)	0.0035(3)	0.3596(2)	0.0192(6)
$C1_X$	-0.255(3)	-0.251(5)	0.300(2)	0.137(18)
$O1_X$	-0.260(2)	-0.298(4)	0.3736(19)	0.124(12)
$O2_X$	-0.245(2)	-0.173(3)	0.2402(17)	0.109(10)
H1	0.300(4)	-0.158(4)	0.569(3)	0.004(9)
H2	0.003(4)	0.292(5)	0.491(3)	0.006(10)
H3	0.138(4)	0.249(4)	0.136(3)	0.008(11)
H4	0.438(5)	0.392(7)	0.460(4)	0.045(17)
H5	0.017(4)	-0.189(5)	0.269(3)	0.008(10)
H6	0.525(5)	-0.040(6)	0.234(4)	0.031(14)

[a]Subscript X indicates CO_2 atoms

Table S3. Anisotropic displacement parameters for CO_2-loaded α-$Zn_3(HCOO)_6$. Errors are given in parentheses.

Atom[a]	u^{11}	u^{22}	u^{33}	u^{12}	u^{13}	u^{23}
Zn1	0.0100(3)	0.0097(3)	0.0098(3)	0.00014(18)	0.00347(19)	0.00060(18)
Zn2	0.0115(3)	0.0101(3)	0.0106(3)	-0.00007(18)	0.00315(19)	0.00103(18)
Zn3	0.0090(4)	0.0147(4)	0.0126(4)	-0.0006(3)	0.0019(3)	0.0013(3)
Zn4	0.0104(4)	0.0134(4)	0.0133(4)	-0.0014(3)	0.0058(3)	0.0016(3)
O1	0.0118(13)	0.0168(14)	0.0127(13)	-0.0019(11)	0.0038(10)	0.0029(11)
C1	0.017(2)	0.013(2)	0.0118(19)	-0.0002(15)	0.0012(16)	0.0031(15)
O2	0.0105(14)	0.0189(15)	0.0223(15)	-0.0013(11)	0.0064(11)	0.0063(11)
O3	0.0128(12)	0.0091(14)	0.0158(13)	0.0012(11)	0.0073(10)	0.0015(11)
C2	0.0116(19)	0.023(2)	0.0124(19)	0.0003(16)	0.0034(16)	0.0006(17)
O4	0.0178(14)	0.0133(15)	0.0182(14)	0.0002(11)	0.0076(11)	0.0023(11)
O5	0.0151(13)	0.0092(14)	0.0119(13)	-0.0010(11)	0.0023(10)	-0.0003(10)
C3	0.0149(18)	0.014(2)	0.0105(18)	0.0024(15)	-0.0011(14)	0.0013(15)
O6	0.0194(14)	0.0126(14)	0.0144(13)	0.0014(11)	-0.0010(11)	-0.0031(11)
O7	0.0104(14)	0.0155(15)	0.0112(14)	0.0007(9)	0.0003(11)	0.0013(10)
C4	0.0155(19)	0.014(2)	0.020(2)	-0.0030(16)	0.0012(16)	-0.0013(17)
O8	0.0174(14)	0.0174(15)	0.0216(15)	0.0012(12)	-0.0034(12)	0.0006(12)
O9	0.0116(13)	0.0124(14)	0.0137(13)	-0.0017(10)	0.0042(10)	-0.0014(10)
C5	0.016(2)	0.017(2)	0.015(2)	-0.0056(16)	0.0040(16)	-0.0033(16)
O10	0.0150(14)	0.0242(16)	0.0178(15)	-0.0058(11)	0.0081(12)	-0.0021(12)

O11	0.0112(13)	0.0114(14)	0.0144(13)	0.0002(10)	0.0047(10)	-0.0025(10)
C6	0.0133(19)	0.018(2)	0.0100(19)	-0.0007(15)	0.0031(15)	0.0005(15)
O12	0.0134(14)	0.0303(18)	0.0140(15)	0.0002(11)	0.0016(11)	0.0017(12)
$C1_X$	0.036(18)	0.26(4)	0.12(2)	0.02(2)	0.020(17)	0.08(3)
$O1_X$	0.071(17)	0.20(3)	0.100(18)	0.01(2)	0.024(14)	0.05(2)
$O2_X$	0.056(13)	0.20(3)	0.074(14)	-0.007(16)	0.000(11)	0.025(16)

[a]Subscript X indicates CO_2 atoms

Table S4. Bond lengths (Å) for CO_2-loaded α-$Zn_3(HCOO)_6$.[a] Errors are given in parentheses.

Zn1-O1	2.034(3)	O1-C1	1.286(5)
Zn1-O3	2.063(3)	C1-O2	1.224(5)
Zn1-O9	2.102(3)	C1-H1	0.89(5)
Zn1-O11	2.108(3)	O3-C2	1.273(5)
Zn1-O5	2.108(3)	C2-O4	1.241(5)
Zn1-O7	2.126(3)	C2-H2	1.00(5)
Zn2-O6[1]	2.033(3)	O5-C3	1.269(5)
Zn2-O4	2.036(3)	C3-O6	1.238(5)
Zn2-O11[1]	2.076(3)	C3-H3	0.97(5)
Zn2-O7	2.105(3)	O6-Zn2[4]	2.033(3)
Zn2-O5	2.134(3)	O7-C4	1.271(5)
Zn2-O9[1]	2.147(3)	C4-O8	1.238(5)
Zn3-O8	2.066(3)	C4-H4	1.03(6)
Zn3-O8[2]	2.066(3)	O9-C5	1.267(5)
Zn3-O12[2]	2.090(3)	O9-Zn2[4]	2.147(3)
Zn3-O12	2.090(3)	C5-O10	1.236(5)
Zn3-O1	2.124(3)	C5-H5	0.92(5)
Zn3-O1[2]	2.124(3)	O11-C6	1.266(5)
Zn4-O10[3]	2.074(3)	O11-Zn2[4]	2.076(3)
Zn4-O10	2.074(3)	C6-O12	1.239(5)
Zn4-O2[3]	2.080(3)	C6-H6	0.96(6)

Zn4-O2	2.080(3)	$C1_X$-$O1_X$	1.161(7)
Zn4-O3	2.116(3)	$C1_X$-$O2_X$	1.161(7)
Zn4-O3[3]	2.116(3)		

1. -x+1/2, y+1/2, -z+1/2

2. 1-x, -y,1+ -z

3. -x, -y,1+ -z

4. -x+1/2,-1+ y+1/2, -z+1/2

[a]Subscript X indicates CO_2 atoms

Table S5. Bond angles (°) for CO_2-loaded α-$Zn_3(HCOO)_6$.[a] Errors are given in parentheses.

O1-Zn1-O3	96.05(10)	O10-Zn4-O3	93.48(10)
O1-Zn1-O9	98.42(11)	$O2^3$-Zn4-O3	88.08(10)
O3-Zn1-O9	96.05(10)	O2-Zn4-O3	91.92(10)
O1-Zn1-O11	89.84(11)	$O10^3$-Zn4-$O3^3$	93.48(10)
O3-Zn1-O11	172.00(11)	O10-Zn4-$O3^3$	86.52(10)
O9-Zn1-O11	77.68(10)	$O2^3$-Zn4-$O3^3$	91.92(10)
O1-Zn1-O5	171.92(10)	O2-Zn4-$O3^3$	88.08(10)
O3-Zn1-O5	88.68(10)	O3-Zn4-$O3^3$	180.0
O9-Zn1-O5	87.55(10)	C1-O1-Zn1	124.3(3)
O11-Zn1-O5	86.11(10)	C1-O1-Zn3	119.9(2)
O1-Zn1-O7	95.07(11)	Zn1-O1-Zn3	115.74(12)
O3-Zn1-O7	93.04(11)	O2-C1-O1	126.2(4)
O9-Zn1-O7	162.82(11)	O2-C1-H1	118(3)
O11-Zn1-O7	91.82(10)	O1-C1-H1	116(3)
O5-Zn1-O7	78.10(10)	C1-O2-Zn4	139.6(3)
$O6^1$-Zn2-O4	94.71(11)	C2-O3-Zn1	128.9(2)
$O6^1$-Zn2-$O11^1$	96.19(10)	C2-O3-Zn4	118.9(2)
O4-Zn2-$O11^1$	92.24(11)	Zn1-O3-Zn4	112.16(12)
$O6^1$-Zn2-O7	94.26(11)	O4-C2-O3	126.8(4)
O4-Zn2-O7	90.75(11)	O4-C2-H2	119(3)
$O11^1$-Zn2-O7	168.86(10)	O3-C2-H2	114(3)
$O6^1$-Zn2-O5	169.75(11)	C2-O4-Zn2	130.2(3)
O4-Zn2-O5	92.10(11)	C3-O5-Zn1	132.5(3)
$O11^1$-Zn2-O5	91.19(10)	C3-O5-Zn2	127.8(2)
O7-Zn2-O5	77.97(10)	Zn1-O5-Zn2	97.22(11)
$O6^1$-Zn2-$O9^1$	88.29(11)	O6-C3-O5	126.6(4)
O4-Zn2-$O9^1$	169.44(11)	O6-C3-H3	121(3)
$O11^1$-Zn2-$O9^1$	77.36(10)	O5-C3-H3	113(3)
O7-Zn2-$O9^1$	99.14(11)	C3-O6-$Zn2^4$	126.8(3)
O5-Zn2-$O9^1$	86.39(10)	C4-O7-Zn2	125.8(3)

O8-Zn3-O8[2]	180.0	C4-O7-Zn1	132.5(3)
O8-Zn3-O12[2]	88.59(11)	Zn2-O7-Zn1	97.57(12)
O8[2]-Zn3-O12[2]	91.42(11)	O8-C4-O7	126.4(4)
O8-Zn3-O12	91.41(11)	O8-C4-H4	118(3)
O8[2]-Zn3-O12	88.58(11)	O7-C4-H4	115(3)
O12[2]-Zn3-O12	180.0	C4-O8-Zn3	132.0(3)
O8-Zn3-O1	91.62(11)	C5-O9-Zn1	133.4(3)
O8[2]-Zn3-O1	88.38(11)	C5-O9-Zn2[4]	126.2(3)
O12[2]-Zn3-O1	84.87(10)	Zn1-O9-Zn2[4]	97.82(10)
O12-Zn3-O1	95.13(10)	O10-C5-O9	127.2(4)
O8-Zn3-O1[2]	88.38(11)	O10-C5-H5	114(3)
O8[2]-Zn3-O1[2]	91.62(11)	O9-C5-H5	119(3)
O12[2]-Zn3-O1[2]	95.13(10)	C5-O10-Zn4	131.3(3)
O12-Zn3-O1[2]	84.87(10)	C6-O11-Zn2[4]	127.6(2)
O1-Zn3-O1[2]	180.0	C6-O11-Zn1	131.6(3)
O10[3]-Zn4-O10	180.0	Zn2[4]-O11-Zn1	99.92(11)
O10[3]-Zn4-O2[3]	91.39(12)	O12-C6-O11	125.9(4)
O10-Zn4-O2[3]	88.61(12)	O12-C6-H6	116(3)
O10[3]-Zn4-O2	88.61(12)	O11-C6-H6	118(3)
O10-Zn4-O2	91.39(12)	C6-O12-Zn3	132.9(3)
O2[3]-Zn4-O2	180.0	$O1_X$-$C1_X$-$O2_x$	163(6)
O10[3]-Zn4-O3	86.52(10)		

1. -x+1/2, y+1/2, -z+1/2

2. 1-x, -y,1+ -z

3. -x, -y,1+ -z

4. -x+1/2,-1+ y+1/2, -z+1/2

[a]Subscript X indicates CO_2 atoms

Table S6. Torsion angles (°) for CO_2-loaded α-$Zn_3(HCOO)_6$. Errors are given in parentheses.

Zn1-O1-C1-O2	-11.3(6)	Zn2-O7-C4-O8	176.3(3)
Zn3-O1-C1-O2	168.1(3)	Zn1-O7-C4-O8	24.6(6)
O1-C1-O2-Zn4	-21.9(7)	O7-C4-O8-Zn3	6.4(7)
Zn1-O3-C2-O4	7.7(6)	Zn1-O9-C5-O10	-14.2(7)
Zn4-O3-C2-O4	-170.5(3)	Zn2[1]-O9-C5-O10	-171.9(3)
O3-C2-O4-Zn2	1.2(6)	O9-C5-O10-Zn4	-8.2(7)
Zn1-O5-C3-O6	-6.2(6)	Zn2[1]-O11-C6-O12	-151.9(3)
Zn2-O5-C3-O6	152.1(3)	Zn1-O11-C6-O12	15.1(6)
O5-C3-O6-Zn2[1]	-6.5(6)	O11-C6-O12-Zn3	19.8(6)

1. -x+1/2,-1+ y+1/2, -z+1/2

Table S7. Potential host-guest hydrogen bonds within CO_2-loaded α-$Zn_3(HCOO)_6$. Errors are given in parentheses.

Hydrogen Bond	D—H (Å)	H···A (Å)	D···A (Å)	D—H···A (°)
C3-H3···O8[1]	0.97(5)	2.62(5)	3.395(5)	137(3)
C4-H4···O6[2]	1.03(6)	2.51(6)	3.162(5)	121(4)
C6-H6···O4[3]	0.96(6)	2.67(5)	3.181(5)	114(4)

1. x-1/2,1+ -y-1/2, z-1/2
2. -x+1/2, y+1/2, -z+1/2
3. -x+1/2,-1+ y+1/2, -z+1/2

Table S8. The average O-Zn-O bond angles (°) and Zn-O distances (Å) in CO_2-loaded α-$Zn_3(HCOO)_6$ and activated $Zn_3(HCOO)_6$ for the four crystallographically inequivalent Zn. Errors are given in parentheses.

	CO_2-loaded α-$Zn_3(HCOO)_6$	Activated $Zn_3(HCOO)_6$[a]
Zn1-O	2.0905 (17)	2.0901 (27)
Zn2-O	2.0892 (17)	2.0885 (27)
Zn3-O	2.0953 (17)	2.0934 (27)
Zn4-O	2.0901 (17)	2.0898 (27)
O-Zn1-O	89.88 (6)	89.87 (10)
O-Zn2-O	90.05 (6)	90.05 (11)
O-Zn3-O	90.00 (6)	90.00 (11)
O-Zn4-O	90.00 (6)	90.00 (11)

[a]Data acquired from reference 1.

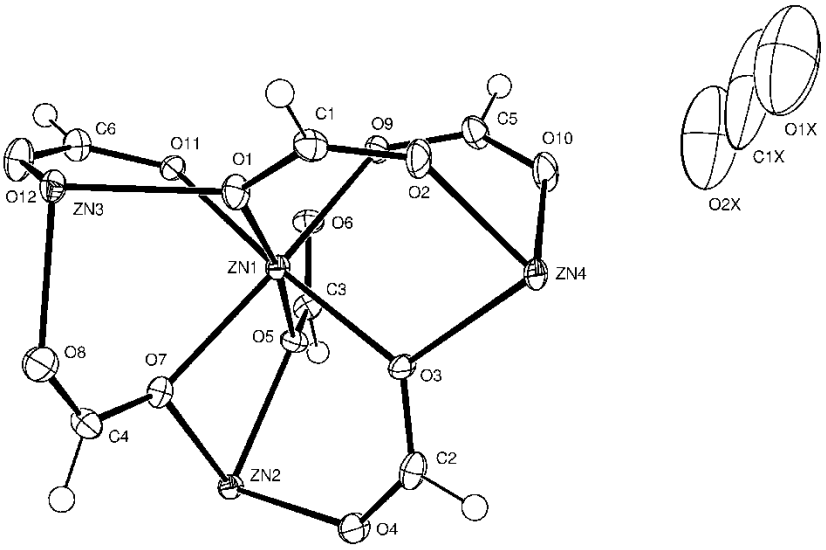

Figure S1. ORTEP drawing of the asymmetric unit of CO_2-loaded α-$Zn_3(HCOO)_6$ at 120 K. Ellipsoids are at the 50% probability level and hydrogens were drawn with arbitrary radii for clarity.

^{67}Zn SSNMR Experimental Procedures

^{67}Zn SSNMR experiments were performed at the National Ultrahigh-Field NMR Facility for Solids (www.nmr900.ca) using a Bruker Avance II NMR spectrometer (B_o = 21.1 T, $\nu_o(^{67}Zn)$ = 56.29 MHz). The static experiments were performed using a home-built 7 mm single-channel static probe. The magic-angle spinning (MAS) experiment was performed using a 4 mm Bruker H/X low gamma MAS probe. For all experiments, external chemical shift referencing and pulse calibration were performed using a 1.0 M aqueous $Zn(NO_3)_2$ solution (δ_{iso} = 0 ppm). All spectra were recorded using a central-transition selective π/2 pulse width of 3 μs, which was determined by scaling the non-selective pulse length by 1/(I + 1/2) where I = 5/2 for ^{67}Zn.

The static SSNMR spectra were acquired for the as-made, activate, CO_2-loaded and CO-loaded MOFs using a solid echo pulse sequence (i.e., $\pi/2 - \tau_1 - \pi/2 - \tau_2$ – acquire) with an inter-pulse delay (τ_1) of 67 μs. For the as-made sample, the recycle delay was set to 0.25 s and 32 k scans were recorded. For the activated, CO_2-loaded and CO-loaded samples, a recycle delay of 1 s was used and 64 K scans were acquired. MAS experiment was also conducted on the as-made sample. A spinning speed of 15 kHz was employed, and the spectrum was obtained using a solid echo pulse sequence (i.e., $\pi/2 - \tau_1 - \pi/2 - \tau_2$ – acquire). An inter-pulse delay (τ_1) of 63.6 μs was used. The recycle delay was set to 0.25 s, and 576 k scans were collected. Data were processed using TopSpin 2.1. The recorded FIDs were left-shifted to the echo maxima when needed.

Computational Details

^{67}Zn magnetic shielding and electric field gradient (EFG) tensors were calculated via the guage-including projector-augmented wave (GIPAW) method using the NMR module of the CASTEP software package[2-5] (version 4.4). The unit cell parameters and atomic coordinates were obtained from the crystal structure of α-$Zn_3(HCOO)_6$·1/3HCO_2H.[6] The solvent molecules were removed, and the resulting structure was geometry optimized by CASTEP. Two types of geometry optimization were performed: (a) the positions of all atoms are optimized and (b) the positions of the linker atoms are optimized and the positions of the metal centers were held fixed. For both geometry optimizations, the generalized gradient approximation functional of Perdew, Burke and Ernzerhof (GGA-PBE) was employed. "Ultrasoft" pseudopotentials, a plane-wave cutoff energy of 294 eV and a (1 x 1 x 1) *k*-point grind were used. The resulting optimized structures were used as inputs for the NMR calculations of the ^{67}Zn magnetic shielding EFG tensors. A plane-wave cutoff energy of 294 eV, a (1 x 1 x 1) *k*-point grind, and "ultrasoft" pseudopotentials generated by the on-the-fly method were employed. The calculated isotropic magnetic shielding values (σ_{iso}) were converted into isotropic chemical shift (δ_{iso}) values using the relation: δ_{iso} [ppm] = 1831.67 ppm - σ_{iso} [ppm], where 1831.67 ppm is the absolute shielding for an infinitely dilute $^{67}Zn^{2+}$ ion in D_2O at 303 K.[7-9] A nuclear quadrupole moment of 122 mb was used to generate the calculated quadrupolar coupling constants (C_Q).[10, 11] The Euler angles between the magnetic shielding and EFG tensors were visualized using MagresView[12] and the theoretical ^{67}Zn SSNMR spectra were plotted using WSolids.[13]

^{67}Zn SSNMR Results

To probe the local environment of the metal centers and the effect of adsorption of guest species on the Zn local structures, static ^{67}Zn SSNMR experiments were performed for the as-made, activated, CO- and CO_2-loaded α-$Zn_3(HCOO)_6$ (Figure S2). The spectra of the four samples look identical, suggesting that the presence of guest species inside the framework does not significantly alter the local Zn environments. This result is consistent with the crystallographic studies which show the Zn local geometry in as-made, the CO_2-loaded and activated frameworks are very similar. Furthermore, the crystal structures of the as-made, activated, and CO_2-loaded α-$Zn_3(HCOO)_6$ indicate that there are four crystallographically inequivalent Zn sites in each phase with very similar local environments. This agrees with the observed ^{67}Zn spectra, which contain multiple ^{67}Zn signals severely overlapping with each other. No attempt was made to separate the individual resonances from different site via spectral simulation. For as-made α-$Zn_3(HCOO)_6$, ^{67}Zn MAS spectrum was also acquired. Only a relatively narrow signal was observed, confirming that the four Zn sites have very similar local structures.

To better understand the observed ^{67}Zn spectra, ^{67}Zn SSNMR parameters were calculated for the activated MOF by the DFT method. Two geometry optimized structures were used for calculation: (a) the positions of all atoms are optimized and (b) only the positions of the linker atoms are optimized and the positions of Zn atoms were held fixed. The calculated ^{67}Zn NMR parameters are summarized in Table S9. For both structures, the absolute quadrupolar coupling constants ($|C_Q|$s) for the four crystallographically inequivalent Zn were calculated to be within the range of ca. 4 to 8 MHz. The calculated asymmetry parameters (η_Q) were non-zero, consistent with the fact that none of the Zn lies on an *n*-fold rotation axis ($n \geq 3$). There are also small, but non-negligible chemical shift anisotropy (CSA) for each site. The calculations suggest that the observed static ^{67}Zn spectra are mainly dominated by the second-order quadrupolar interaction with a minor contribution from the CSA.

The calculations based on the structure (a) indicate Zn1 and Zn2 have smaller C_Q values, whereas the structure (b) predicts that Zn1 has the largest C_Q. Comparisons of the theoretical static and MAS spectra with the experimental ones suggest that the calculated ^{67}Zn spectra based on structure (b) match the observed spectra slightly better. This implies that the geometrically optimized structure involving only the linker atoms more closely resembles the real structure. It appears that the broad “feet” in the static spectrum of the activated phase with a breath of ca. 50 kHz is due to Zn1.

Table S9. The calculated ^{67}Zn EFG and chemical shift (CS) tensor parameters, and the Euler angles (α, β, γ) describing the orientation of the CS and EFG principal axis systems for the four crystallographically inequivalent Zn atoms (Zn1, Zn2, Zn3 and Zn4) in the activated α-$Zn_3(HCOO)_6$ MOF.[a]

Geometry Optimization Performed on All Atoms[a]								
	δ_{iso} (ppm)	Ω (ppm)	κ	$\lvert C_Q \rvert$[c] (MHz)	η_Q	α [°]	β [°]	γ [°]
Zn1	297.1	46.2	-0.30	5.1	0.96	33	70	-1
Zn2	321.1	101.1	0.22	4.3	0.11	-61	59	41
Zn3	288.4	69.1	-0.03	8.2	0.39	94	154	4
Zn4	293.5	94.1	0.50	6.9	0.95	69	153	-82
Geometry Optimization Performed on Linker Atoms[b]								
	δ_{iso} (ppm)	Ω (ppm)	κ	$\lvert C_Q \rvert$[c] (MHz)	η_Q	α [°]	β [°]	γ [°]
Zn1	300.2	53.3	-0.09	7.4	0.62	119	21	-123
Zn2	321.9	92.3	0.30	4.4	0.76	63	132	-135
Zn3	273.6	83.2	0.50	4.6	0.77	172	154	105
Zn4	299.5	76.0	0.92	5.5	0.93	135	150	-109

[a]The input structure was obtained from the unit cell parameters and atomic coordinate of α-$Zn_3(HCOO)_6 \cdot 1/3HCO_2H$.[6] The solvent molecules were removed, and the positions of all atoms were geometry optimized.

[b]The input structure was obtained from the unit cell parameters and atomic coordinate of α-$Zn_3(HCOO)_6 \cdot 1/3HCO_2H$.[6] The solvent molecules were removed, and the positions of the linker atoms were geometry optimized.

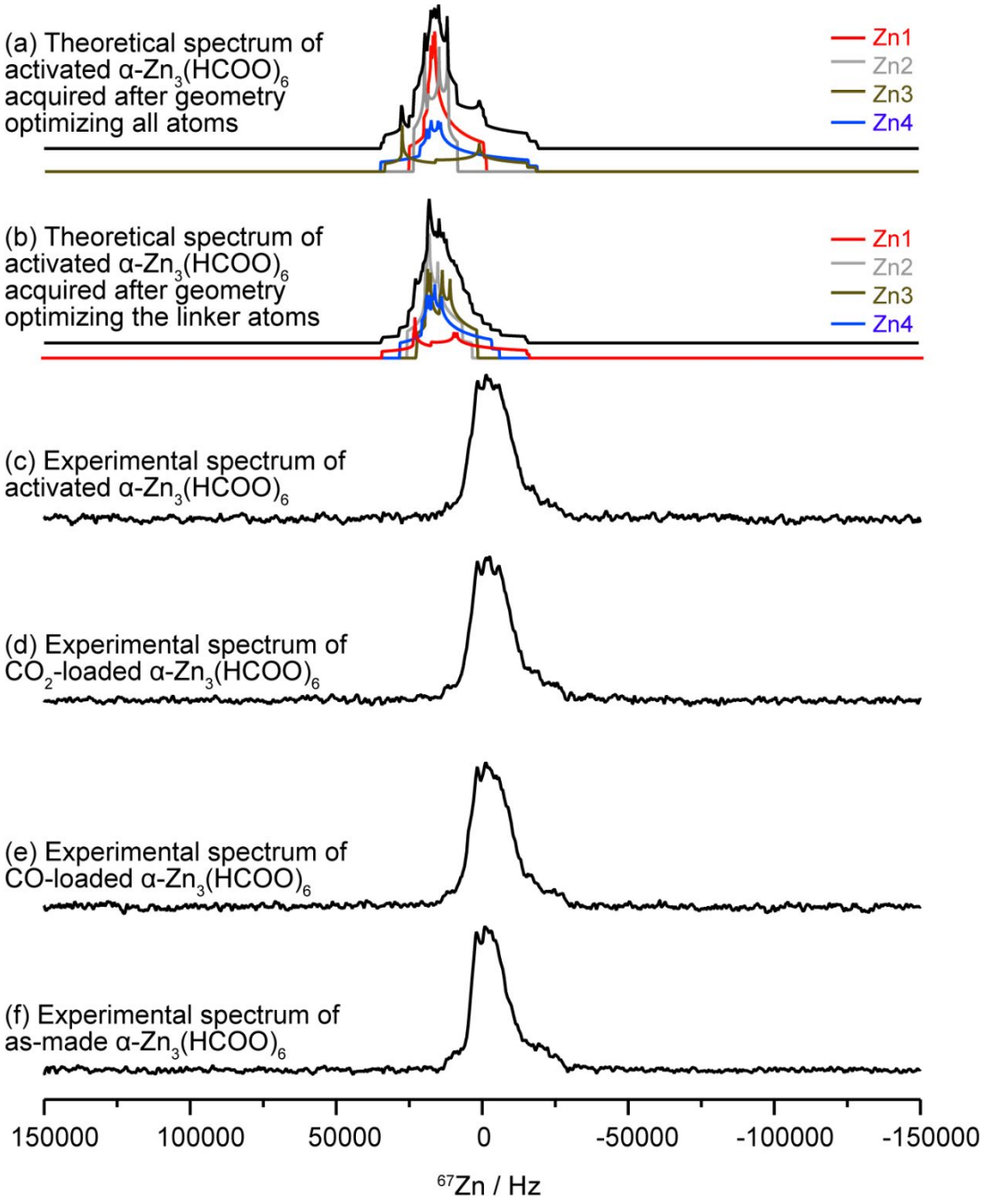

Figure S2. (a and b) The theoretical static ^{67}Zn SSNMR spectra of activated α-$Zn_3(HCOO)_6$ shown as summations (black trace) of the Zn1 (red trace), Zn2 (gray trace), Zn3 (brown trace) and Zn4 (blue trace) resonances. (a) was acquired after geometry optimizing the positions of all atoms, while (b) was acquired after geometry optimizing the positions of the linker atoms. The calculated EFG and CS tensor parameters are also provided in Table S9. The experimental static ^{67}Zn SSNMR spectra of (c) activated, (d) CO_2-loaded, (e) CO-loaded and (f) as-made α-$Zn_3(HCOO)_6$ acquired at 21.1 T.

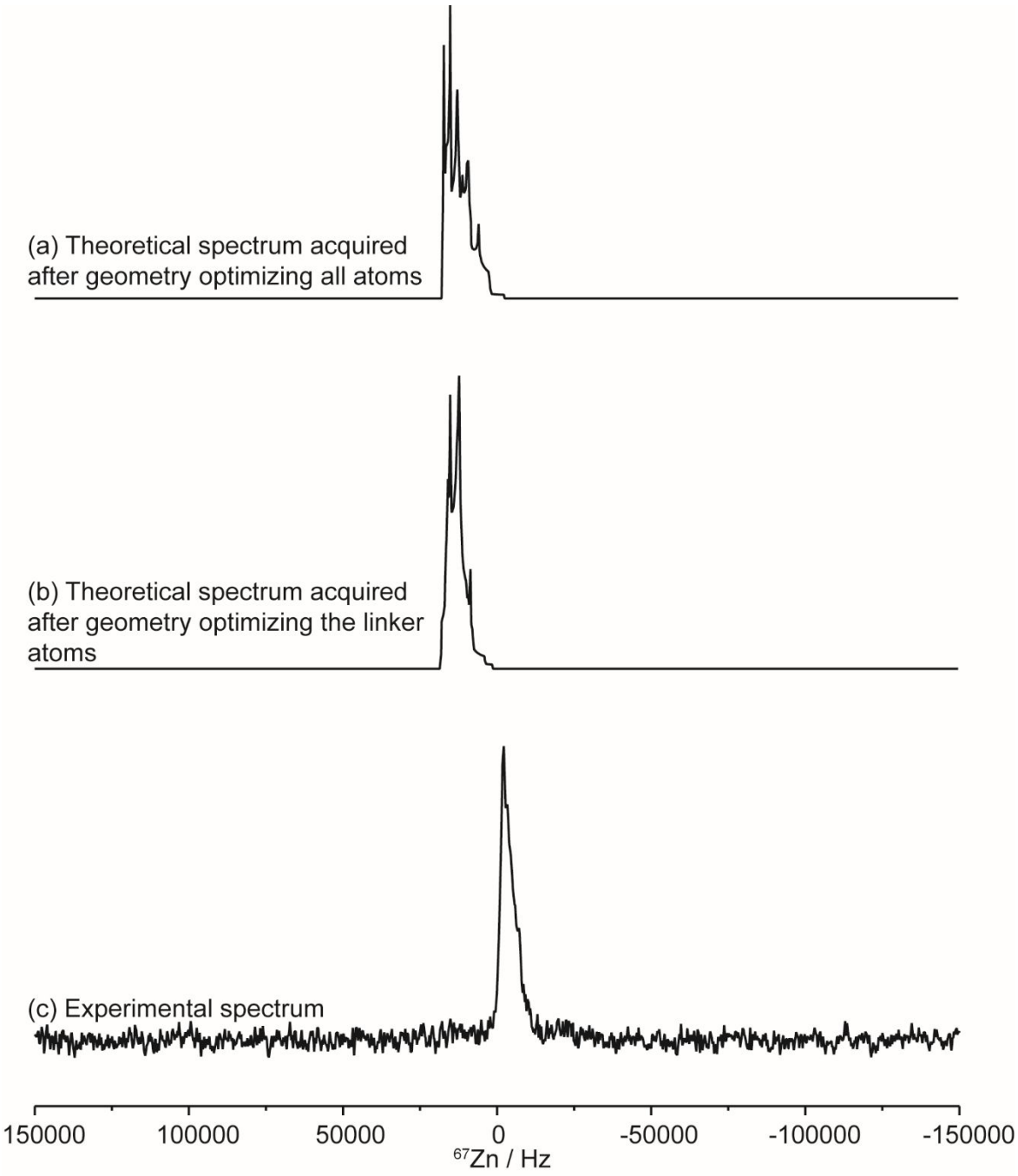

Figure S3. Theoretical (a and b) and experimental (c) ^{67}Zn SSNMR spectra of as-made α-$Zn_3(HCOO)_6$. (a) was acquired after geometry optimizing the positions of all atoms, while (b) was acquired after geometry optimizing the positions of the linker atoms. The experimental spectrum was acquired at 15 kHz and 21.1 T.

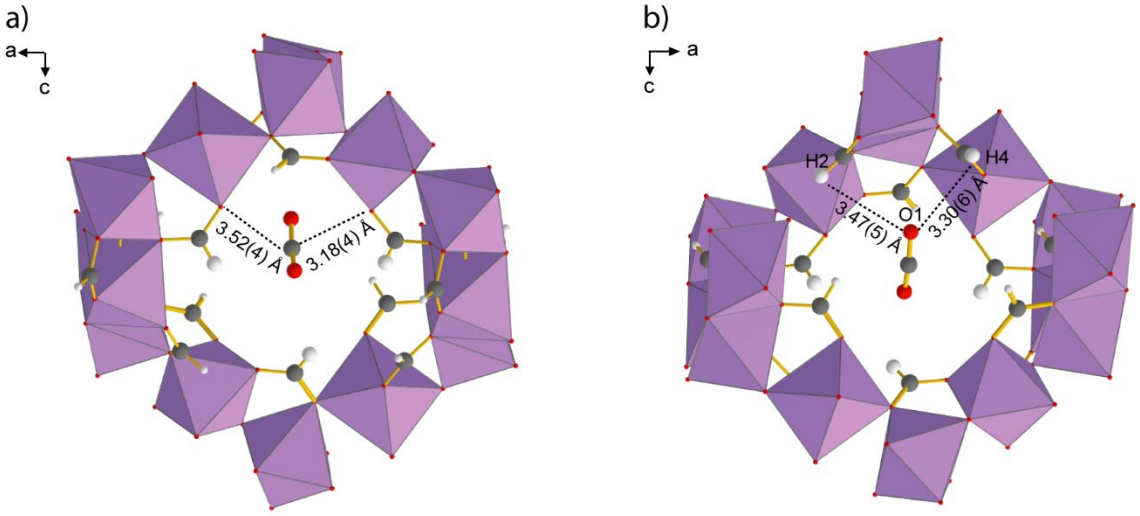

Figure S4. The local pore structure of CO_2-loaded α-$Zn_3(HCOO)_6$, as viewed from different perspectives. (a) Shows the distances between the carbon of the CO_2 and the closest framework oxygens, while (b) shows the distance between one of the oxygens (O1) of CO_2 and two closest framework hydrogens (H2 and H4). Carbons are grey, oxygens are red, hydrogens are white and [ZnO_6] units are depicted as purple octahedra. Errors associated with the distances are provided in parentheses.

Table S10. The apparent ^{13}C CS tensor parameters (δ_{iso}, Ω and κ) and motional angles (α and β) of CO_2 adsorbed in α-$Zn_3(HCOO)_6$ at temperatures ranging from 123 to 433 K. The CS tensor parameters were obtained from analytical simulations, and the angles were acquired from motional simulations. All motions occur at rates on the order of magnitude of ca. ≥ 10^7 Hz in the considered temperature range.

Temperature [K]	δ_{iso} [ppm]	Ω [ppm]	κ	α [°]	β [°]
433	126.0 ± 1.0	36.3 ± 2.0	-0.42 ± 0.02	47.5 ± 0.5	40.0 ± 0.5
413	126.5 ± 0.5	35.5 ± 1.0	-0.38 ± 0.05	47.5 ± 0.5	39.0 ± 0.5
393	126.3 ± 0.5	34.0 ± 0.5	-0.38 ± 0.05	47.5 ± 0.5	39.0 ± 0.5
373	126.1 ± 0.5	32.0 ± 0.5	-0.46 ± 0.02	48.0 ± 0.5	40.0 ± 0.5
353	126.2 ± 0.5	29.5 ± 0.5	-0.51 ± 0.02	48.0 ± 0.5	40.0 ± 0.5
333	126.3 ± 0.5	27.7 ± 0.5	-0.61 ± 0.03	49.0 ± 0.5	41.5 ± 0.5
313	126.2 ± 0.5	24.5 ± 0.5	-0.76 ± 0.02	49.5 ± 0.5	43.5 ± 0.5
293	126.2 ± 0.5	22.5 ± 0.5	-0.96 ± 0.02	49.5 ± 0.5	47.0 ± 0.5
273	126.2 ± 0.5	23.0 ± 1.0	-0.74 ± 0.02	49.5 ± 0.5	42.5 ± 0.5
253	126.0 ± 0.5	26.5 ± 1.0	-0.40 ± 0.02	49.0 ± 0.5	39.5 ± 0.5
233	125.9 ± 0.5	32.0 ± 1.0	-0.02 ± 0.02	49.0 ± 0.5	36.0 ± 0.5
213	125.7 ± 0.5	40.5 ± 1.0	0.21 ± 0.02	48.0 ± 0.5	32.0 ± 0.5
193	125.5 ± 0.5	53.0 ± 1.0	0.37 ± 0.02	47.0 ± 0.5	30.5 ± 0.5
173	126.3 ± 0.5	70.0 ± 1.0	0.46 ± 0.02	44.0 ± 0.5	28.6 ± 0.5
153	125.5 ± 0.5	89.8 ± 1.0	0.53 ± 0.02	42.0 ± 0.5	26.0 ± 0.5
133	125.5 ± 0.5	112.0 ± 1.0	0.56 ± 0.02	40.0 ± 0.5	24.5 ± 0.5
123	125.5 ± 0.5	128.0 ± 1.0	0.55 ± 0.02	37.0 ± 0.5	25.0 ± 0.5

Table S11. The observed ^{13}C CS tensor parameters (δ_{iso}, Ω and κ) and motional angles (α and β) of CO adsorbed in α-$Zn_3(HCOO)_6$ at various temperatures (T = 173 to 433 K). The ^{13}C CS tensor parameters and the motional angles were obtained from analytical and motional simulations, respectively. All motions occur at rates on the order of magnitude of ca. ≥ 10^7 Hz in the experimental temperature range.

Temperature [K]	δ_{iso} [ppm]	Ω [ppm]	κ	α [°]	β [°]
433	184.0 ± 0.5	41.0 ± 2.0	-0.40 ± 0.05	47.5 ± 0.5	39.5 ± 0.5
413	183.3 ± 0.5	43.0 ± 2.0	-0.30 ± 0.05	47.0 ± 0.5	38.5 ± 0.5
393	184.0 ± 0.5	46.0 ± 2.0	-0.25 ± 0.05	47.0 ± 0.5	37.5 ± 0.5
373	184.0 ± 0.5	46.0 ± 2.0	-0.15 ± 0.05	46.5 ± 0.5	37.0 ± 0.5
353	183.3 ± 0.5	48.0 ± 1.0	-0.05 ± 0.05	46.5 ± 0.5	35.5 ± 0.5
333	183.0 ± 0.5	49.8 ± 1.0	-0.02 ± 0.05	46.5 ± 0.5	35.5 ± 0.5
313	183.0 ± 0.5	50.5 ± 1.0	0.05 ± 0.02	46.5 ± 0.5	35.0 ± 0.5
293	184.0 ± 0.5	56.0 ± 1.0	0.32 ± 0.02	46.0 ± 0.5	29.5 ± 0.5
273	184.0 ± 0.5	58.5 ± 1.0	0.44 ± 0.02	46.0 ± 0.5	28.0 ± 0.5
233	183.6 ± 0.5	65.0 ± 1.0	0.66 ± 0.02	46.0 ± 0.5	23.0 ± 0.5
213	184.0 ± 0.5	65.0 ± 1.0	1 – 0.02	46.0 ± 0.5	20.0 ± 0.5
193	184.0 ± 0.5	70.0 ± 1.0	1 – 0.02	45.5 ± 0.5	20.0 ± 0.5
173	183.0 ± 0.5	77.0 ± 1.0	1 – 0.02	45.0 ± 0.5	20.0 ± 0.5

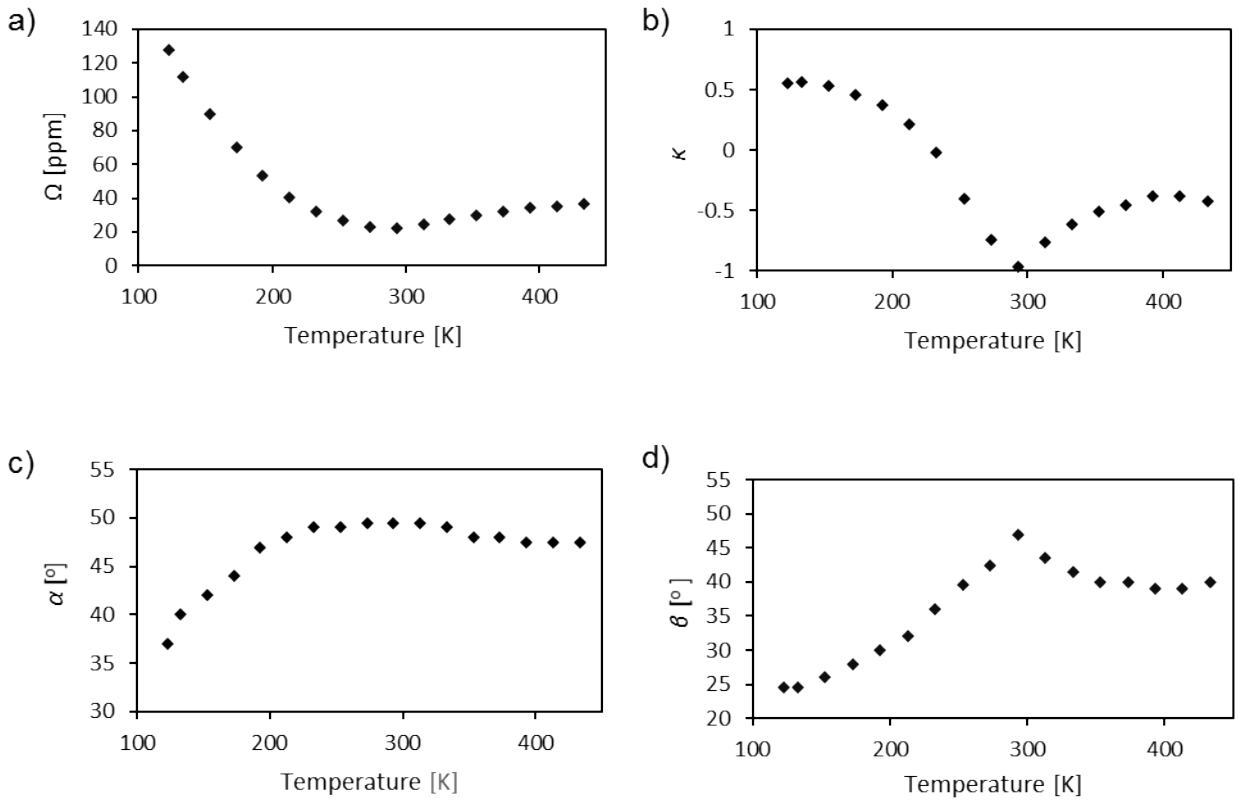

Figure S5. Charts illustrating changes in the (a and b) apparent ^{13}C CS tensor parameters (Ω and κ) and (c and d) motional angles (α and β) of CO_2 adsorbed in α-$Zn_3(HCOO)_6$ as a function of temperature. The values are also tabulated in Table S10.

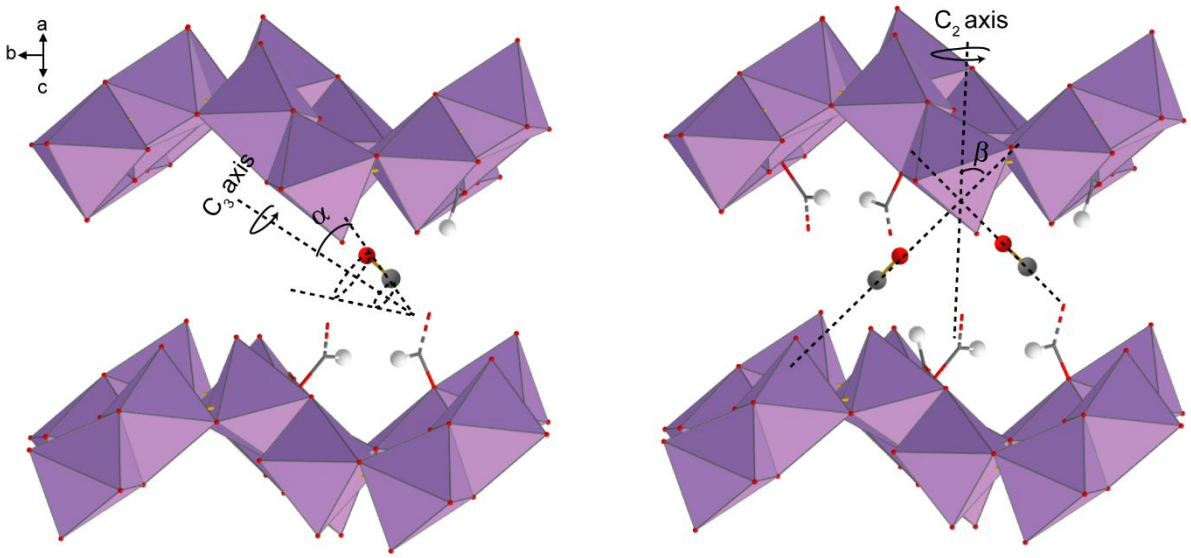

Figure S6. Illustration of the (left) wobbling and (right) hopping motions exhibited by CO in α-$Zn_3(HCOO)_6$. *α* and *β* describe the wobbling and hopping angles, respectively. Carbons are dark grey, oxygens are red, hydrogens are white and [ZnO_6] units are purple octahedra. The [ZnO_6] units that connect the top and the bottom of the channels were omitted for clarity. The red and grey dashed lines represent C-O bonds between the carbons and the omitted [ZnO_6] units. All framework carbons and hydrogens are also omitted for clarity except for H1, H5 and H6 and the corresponding carbons.

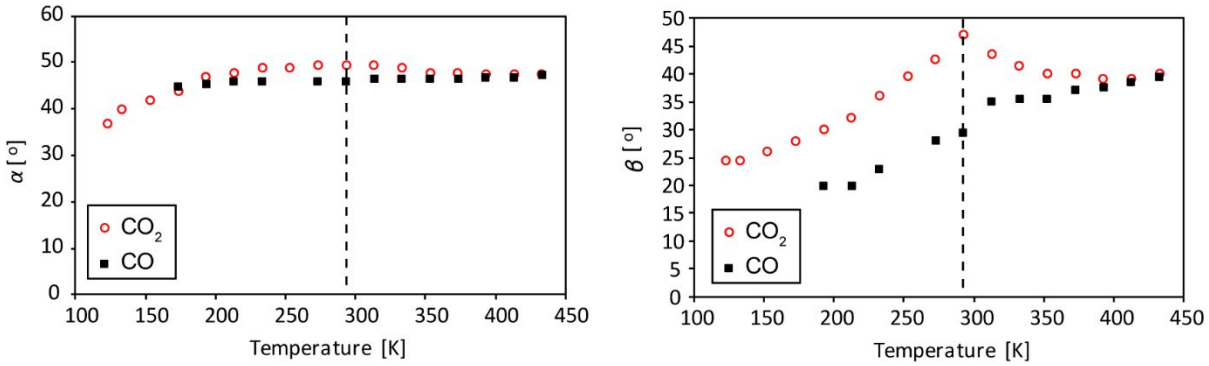

Figure S7. A comparison between the motional angles (α and β) of CO_2 (open red circles) and CO (solid black squares) in α-$Zn_3(HCOO)_6$ at various temperatures. The temperature where the α and β trends begin to reverse for CO_2 (ca. 293 K) is marked with a solid dashed line. α and β were acquired via motional simulations as shown in Figures 4 and 9. The values are also given in Tables S10 and S11.

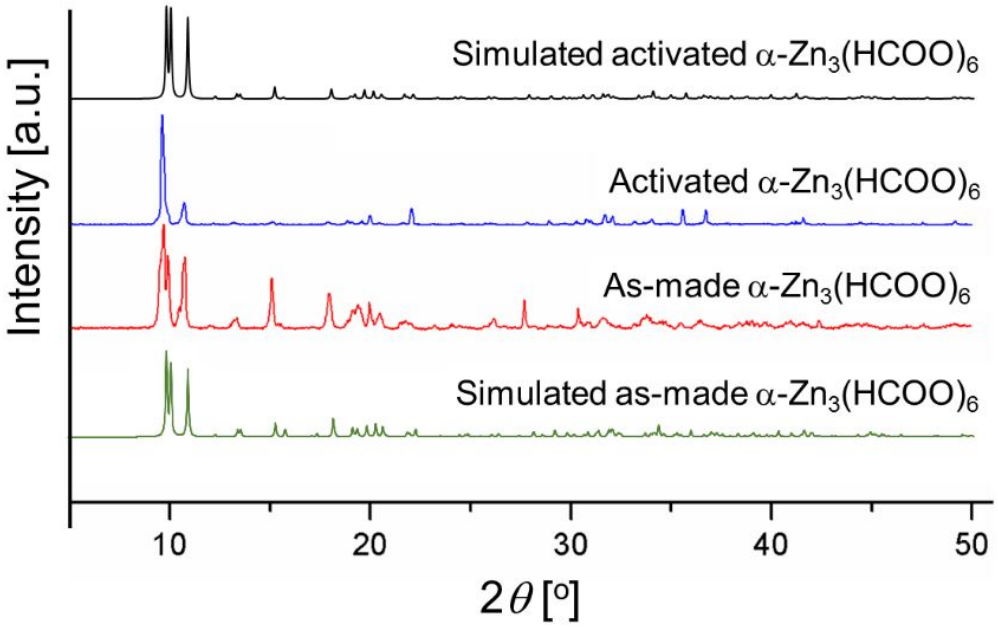

Figure S8. Experimental PXRD patterns of as-made (red trace) and activated (blue trace) α-$Zn_3(HCOO)_6$ and the corresponding theoretical PXRD patterns (black trace for activated, green trace for as-made) constructed using previously reported crystal structures.[1]

The Influence of Temperature on the Motional Rates of CO_2 in α-$Zn_3(HCOO)_6$

Figure S9 shows the spectra simulated for CO_2 in α-$Zn_3(HCOO)_6$ using a wobbling angle of 47.5° and a hopping angle of 40.0°. The simulated spectrum using rates of ca. ≥ 10^7 Hz for both motions is in excellent agreement with the experimental spectrum acquired at 433 K (see Figure 4). Thus, CO_2 undergoes a 47.5° wobbling and a 40.0° hopping at rates of ca. ≥ 10^7 Hz at 433 K. A decrease in temperature can result in a decrease in motional rates; however, we were unable to reproduce the experimental spectra acquired at T < 433 K using the same motional angles at slower motional rates. The experimental spectra were only successfully reproduced when the motional angles were varied with the motions occurring at ca. ≥ 10^7 Hz. Thus, a decrease in temperature results in a change in the motional angles instead of motional rates.

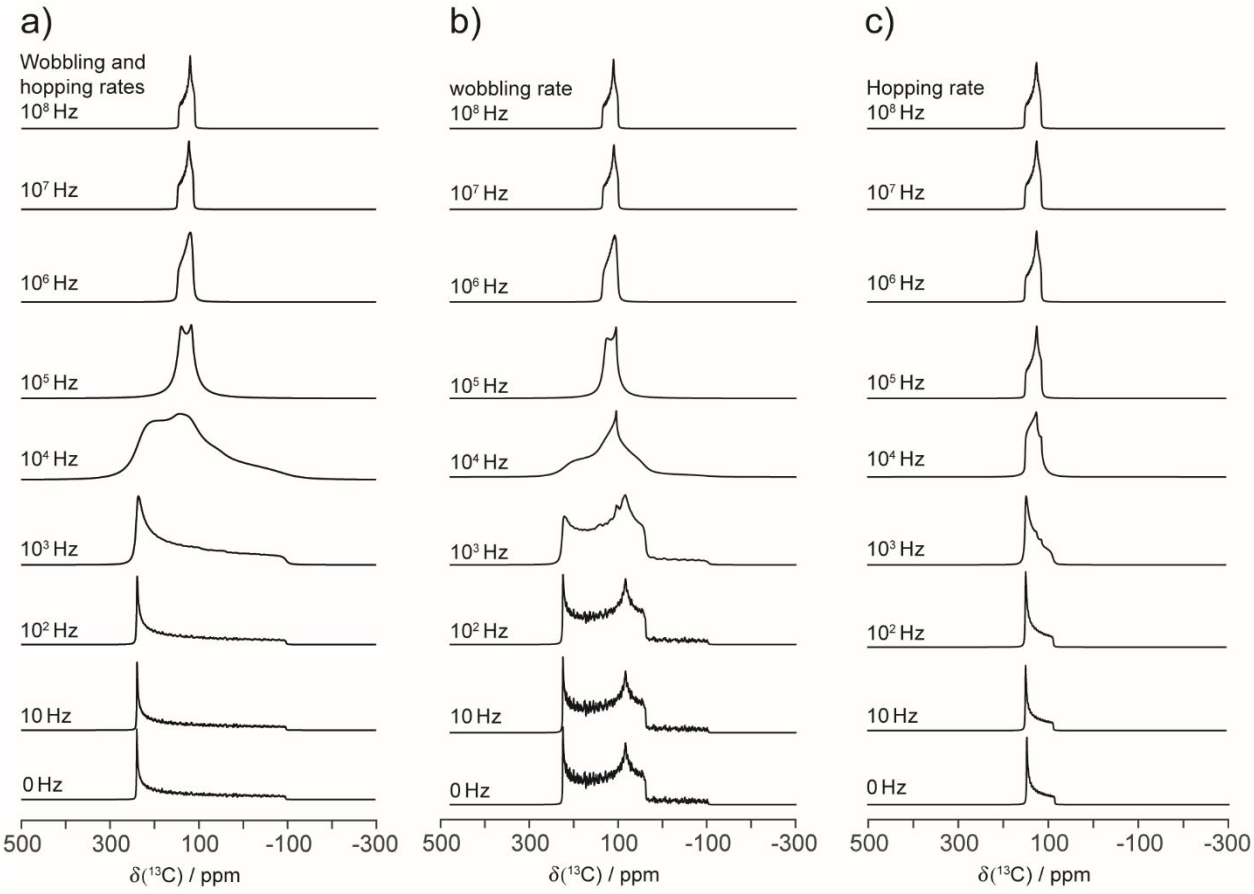

Figure S9. Static $^{13}CO_2$ SSNMR spectra modelled using different motional rates. (a) The wobbling and hopping rates were varied from 0 to 10^8 Hz. (b) The hopping rate was fixed at 10^7Hz while the wobbling rate was varied from 0 to 10^8 Hz. (c) The wobbling rate was fixed at 10^7 Hz while the hopping rate was varied from 0 to 10^8 Hz. Note in (a), (b), and (c), no change in lineshape was observed at rates ≳ 10^7 Hz. All spectra were simulated using a wobbling angle of 47.5° and a hopping angle of 40.0°.

References

(1) Wang, Z.; Zhang, Y.; Kurmoo, M.; Liu, T.; Vilminot, S.; Zhao, B.; Gao, S. $[Zn_3(HCOO)_6]$: A Porous Diamond Framework Conformable to Guest Inclusion. *Aust. J. Chem.* **2006,** *59,* 617-628.

(2) Pickard, C. J.; Mauri, F. All-electron Magnetic Response with Pseudopotentials: NMR Chemical Shifts. *Phys. Rev. B* **2001,** *63,* 245101.

(3) Yates, J. R.; Pickard, C. J.; Mauri, F. Calculation of NMR Chemical Shifts for Extended Systems Using Ultrasoft Pseudopotentials. *Phys. Rev. B* **2007,** *76,* 024401.

(4) Profeta, M.; Mauri, F.; Pickard, C. J. Accurate First Principles Prediction of ^{17}O NMR Parameters in SiO_2: Assignment of the Zeolite Ferrierite Spectrum. *J. Am. Chem. Soc.* **2003,** *125,* 541-548.

(5) Clark, S. J.; Segall, M. D.; Pickard, C. J.; Hasnip, P. J.; Probert, M. I. J.; Refson, K.; Payne, M. C. First Principles Methods Using CASTEP. *Z. Kristallogr.* **2005,** *220,* 567-570.

(6) Viertelhaus, M.; Adler, P.; Clérac, R.; Anson, C. E.; Powell, A. K. Iron(II) Formate $[Fe(O_2CH)_2]\cdot 1/3HCO_2H$: A Mesoporous Magnet − Solvothermal Syntheses and Crystal Structures of the Isomorphous Framework Metal(II) Formates $[M(O_2CH)_2]\cdot n$(Solvent) (M = Fe, Co, Ni, Zn, Mg). *Eur. J. Inorg. Chem.* **2005,** *2005,* 692-703.

(7) *Multinuclear NMR*; Mason, J., Ed.; Plenum Press: New York, 1987.

(8) *Encyclopedia of Nuclear Magnetic Resonance*; Grant, D. M.; Harris Robin, K., Eds.; Wiley: Chichester, 1996; Vol. 2.

(9) Mroué, K. H.; Power, W. P. High-Field Solid-State ^{67}Zn NMR Spectroscopy of Several Zinc−Amino Acid Complexes. *J. Phys. Chem. A* **2010,** *114,* 324-335.

(10) Leroy, C.; Szell, P. M. J.; Bryce, D. L. On the Importance of Accurate Nuclear Quadrupole Moments in NMR Crystallography. *Magn. Reson. Chem.* **2018,** DOI: 10.1002/mrc.4787.

(11) Pyykkö, P. Year-2017 Nuclear Quadrupole Moments. *Mol. Phy.* **2018,** *116,* 1328-1338.

(12) Sturniolo, S.; Green, T. F. G.; Hanson, R. M.; Zilka, M.; Refson, K.; Hodgkinson, P.; Brown, S. P.; Yates, J. R. Visualization and Processing of Computed Solid-state NMR Parameters: MagresView and MagresPython. *Solid State Nucl. Magn. Reson.* **2016,** *78,* 64-70.

(13) Eichele, K. *WSolids*, 1.20.21; University of Tübingen: Germany, 2013.